Magnetic hysteresis based on dipolar interactions in granular magnetic systems

Paolo Allia

*Dipartimento di Fisica, Politecnico di Torino, and INFM, Research Unit Torino Politecnico, Corso Duca degli Abruzzi 24,
I-10129 Torino, Italy*

Marco Coisson

Dipartimento di Elettronica, Politecnico di Torino, Corso Duca degli Abruzzi 24, I-10129 Torino, Italy

Marcelo Knobel

Instituto de Fisica Gleb Wataghin, UNICAMP, C.P. 6165, 13083-970, Campinas, São Paulo, Brazil

Paola Tiberto and Franco Vinai

*Istituto Elettrotecnico Nazionale Galileo Ferraris and INFM, Research Unit Torino Politecnico, Corso Massimo d'Azeglio 42,
I-10125 Torino, Italy*

(Received 28 April 1999)

The magnetic hysteresis of granular magnetic systems is investigated in the high-temperature limit ($T \gg$ blocking temperature of magnetic nanoparticles). Measurements of magnetization curves have been performed at room temperature on various samples of granular bimetallic alloys of the family $Cu_{100-x}Co_x$ ($x = 5$–20 at. %) obtained in ribbon form by planar flow casting in a controlled atmosphere, and submitted to different thermal treatments. The loop amplitude and shape, which are functions of sample composition and thermal history, are studied taking advantage of a novel method of graphical representation, particularly apt to emphasize the features of thin, elongated loops. The hysteresis is explained in terms of the effect of magnetic interactions of the dipolar type among magnetic-metal particles, acting to hinder the response of the system of moments to isothermal changes of the applied field. Such a property is accounted for in a mean-field scheme, by introducing a memory term in the argument of the Langevin function which describes the anhysteretic behavior of an assembly of noninteracting superparamagnetic particles. The rms field arising from the cumulative effect of dipolar interactions is linked by the theory to a measurable quantity, the reduced remanence of a major symmetric hysteresis loop. The theory's self-consistence and adequacy have been properly tested at room temperature on all examined systems. The agreement with experimental results is always striking, indicating that at high temperatures the magnetic hysteresis of granular systems is dominated by interparticle, rather than single-particle, effects. Dipolar interactions seem to fully determine the magnetic hysteresis in the high-temperature limit for low Co content ($x \leq 10$). For higher concentrations of magnetic metal, the experimental results indicate that additional hysteretic mechanisms have to be introduced. [S0163-1829(99)01037-1]

I. INTRODUCTION

Granular magnetic systems are formed by magnetic grains or clusters whose size is of the order of a few nanometers, embedded in a nonmagnetic (insulating or metallic) matrix. The ultrafine solid particles can be obtained by several preparation methods (vapor deposition, sputtering, melt-spinning, electrodeposition, mechanical alloying),[1,2] and the final nanostructure can be usually tailored by specific thermal treatments (either in furnace or by Joule heating).[3] The reduced particle size, combined with specific nanostructures, provides the granular systems with a rich variety of interesting physical properties, which can be subsequently applied in a varied number of applications (playing a fundamental role in the area of magnetic recording).[1,2] Besides their obvious technological relevance, these systems provide a unique setting to investigate several basic aspects of solid-state physics, such as superparamagnetism,[4–6] kinetics of crystal nucleation and growth,[7,8] spin-glass behavior.[9,10] In the last few years, the interest in granular systems has been reinforced by the discovery of the so-called giant magnetoresistance effect,

occurring when the granular structure is composed of two metallic elements (e.g., Fe-Ag, Cu-Co).[3,11] More recently, other systems such as metal-insulator nanocomposites have also shown interesting magnetotransport properties, as tunnel magnetoresistance[12] and giant Hall effect.[13] Owing to the inherent complexity of the nanostructure, the physical response of such systems is very difficult to model and predict. Therefore, although granular magnetic systems have been intensively studied during the last decades, they still present many striking features which remain unexplained.

Let us consider the magnetic properties of an assembly of noninteracting magnetic particles (with a broad distribution of sizes and shapes, and randomly distributed easy axes), which can be studied in the framework of the well-known superparamagnetic model.[14] The first assumption of the superparamagnetic theory is that the atomic magnetic moments within a particle move coherently, and therefore the magnetic moment can be represented by a single classical vector of magnitude $\mu = \mu_{at} \cdot N$, where μ_{at} is the atomic magnetic moment and N is the number of magnetic atoms in the particle. In the simplest case, the magnetic-moment direction is

determined by a uniaxial anisotropy (of crystalline, or shape, or elastic origin) and by an external magnetic field. Each particle has a characteristic relaxation time, which is essentially the average time to reverse its magnetic moment from one equilibrium state to the other. The relaxation time τ is determined by a characteristic attempt frequency (of the order of 10^{10} Hz), and by a Boltzmann factor $\exp(-E/kT)$, where k is the Boltzmann constant, T is temperature, and E is the effective energy barrier which separates the two equilibrium states. This energy barrier is given by the product of the particle volume times the anisotropy energy density K of the particle. If $kT \gg E$ (high T or small volumes), τ turns out to be much shorter than the standard measuring time, and the particle is in the superparamagnetic state. On the other hand, if $kT \ll E$, τ becomes much larger than any observation time, and the particle magnetization remains blocked in the same local energy minimum, so that the particle is known as blocked. For a specific measurement time it is possible to define a temperature which separates both regimes, known as the blocking temperature T_B. It is worth noting that the complexity of the problem makes exact solutions possible only in few limiting cases, such as $T=0$ K for fully blocked particles (Stoner-Wohlfarth model[15]), or $T \gg T_B$ (fully superparamagnetic limit).[5,16] The systems become even more complicated when one takes into account the interactions among the magnetic entities, which have been undoubtedly found in different physical systems by using several experimental techniques.[3,4,9,17,18] Only recently, with the enormous development of computers and important advances of the techniques of statistical physics, realistic multiparticle systems could be reliably simulated using Monte Carlo techniques.[19–24] In this case, there are many simulation models which make use of different approaches and approximations, and therefore the literature is full of inconclusive and/or conflicting results. However, recent investigations agree that magnetostatic interaction produces an increase in T_B, in agreement with experimental findings[19,21] (with an important exception measured by Morup and Tronc[4]). Also, it was found that dipolar interactions cause a slower decay of the remanence and coercivity with temperature.[21] Therefore, there is much evidence that the interactions among magnetic entities can play a fundamental role in the magnetic behavior of granular systems, and can even be responsible for the hysteresis loops measured at room temperature.

In this paper we introduce an analytical theory to describe magnetic hysteresis arising exclusively from interaction effects in granular magnetic systems. The introduction of a memory function, which depends on the initial magnetic state of the sample, brings about some simple consequences, and the problem is solved within the framework of a sort of mean-field approximation. The theory will be first developed for an assembly of identical superparamagnetic moments. Extension to the case of distributed superparamagnetic moments is, however, straightforward, because the moments are treated as statistically independent in a mean-field approach. Most impressive is that the theory allows one to fit experimental curves with a high degree of accuracy, with only one adjustable parameter, namely the mean field resulting from the total long-range interactions within the sample. For the sake of simplicity (and to avoid discrepancies due to intrinsic characteristics of different systems), in this paper we focus only on experimental results obtained from melt-spun Cu-Co ribbons at room temperature. However, we believe that our theoretical considerations can be extended to any granular system which consists of small magnetic particles (''small'' meaning here that the system would behave as a standard superparamagnet if the interactions were not present). In these categories one can find several artificially prepared systems, such as metallic granular solids, metal-insulator composites (cermets), hybrid compounds, frozen ferrofluids, and even many biological and geological systems, such as soil, rocks, and blood.[25] Furthermore, in principle, the theory can be also applied to nanocrystalline systems displaying two phases which are ferromagnetic at room temperature, but can result in a ferromagnetic granular system above the Curie temperature of the interfacial phase. In this family one can include extremely soft magnetic materials, such as Fe-Cu-Nb-Si-B (Ref. 26) or Fe-Zr-B-Cu,[27] and hard magnetic materials, such as the so-called spring-exchange magnets in the high-temperature limit.[28]

II. EXPERIMENTAL

Continuous ribbons of $Cu_{100-x}Co_x$ ($x=5,10,15,20$ at. %) were obtained by planar flow casting in He atmosphere on a Cu-Zr wheel. The quenching parameters were controlled during the rapid solidification process for all studied compositions in order to get comparable quenching rates. Different ribbon strips of the four compositions (width 5×10^{-3} m, thickness $4–6 \times 10^{-5}$ m) were submitted to dc joule heating in vacuum, in order to change the number and size of Co particles, as discussed in Ref. 3. dc joule heating is a technique of fast annealing, where the temperature of a metallic sample is rapidly increased by the heat released by a constant electrical current. Heating rates of the order $10^2–10^3$ K/s are routinely obtained.[29] During each treatment, the samples were clipped between two copper electrodes (fixed sample length: 0.1 m), and submitted to a direct current (in the range 1 A $\leq I \leq 10$A) for a fixed time ($t = 60$ s). All samples submitted to joule heating will be identified by the symbol JH followed by the value of the annealing current.

Magnetization curves were obtained at room temperature on both as-quenched and annealed ribbon strips. The magnetic moment was measured up to 10 kOe using a vibrating-sample magnetometer (LDJ, model 9500). The sample weight was determined by a high-precision electronic balance. Symmetric hysteresis loops were obtained starting from the demagnetized state (reached through ac sample demagnetization) and increasing the applied field to a vertex-field value $+H_V$ ranging between 1×10^2 Oe and 1×10^4 Oe. The hysteretic magnetization was then measured between $\pm H_V$ by changing the measurement field at intervals of the order of one-hundredth of the vertex-field value, to get a high resolution and to keep the number of experimental points invariant with H_V. The low-field region of loops starting from vertex-field values higher than 5×10^3 Oe was carefully investigated by further increasing the number of measurements. The overall time for a closed loop to be completed was of the order of 120 s.

Anhysteretic magnetization curves were obtained as the loci of the cusps of sequential symmetric loops performed up
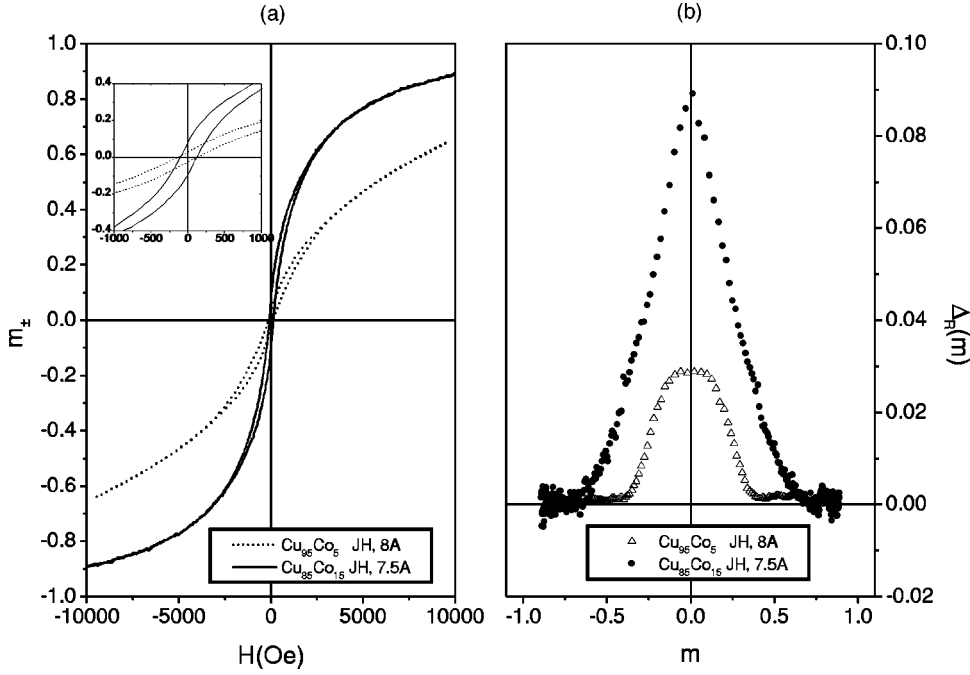
FIG. 1. Representative room-temperature hysteresis loops of two selected $Cu_{100-x}Co_x$ samples, shown in the $m_{\pm}$ vs H representation (a) and in the Δ_R vs m representation (b); m is the reduced magnetization.

to H_V values progressively increasing from 1×10^2 Oe to 1×10^4 Oe. Asymmetric loops leading to the demagnetized state were measured starting from $H_V = +1 \times 10^4$ Oe and progressively reducing, in a controlled way, the values of both negative and positive vertex-field values.

The analysis of hysteresis loops was performed using a method of graphical representation, specifically introduced to make clear and more apparent the features of narrow, elongated hysteresis loops, like the ones found in granular systems [Fig. 1(a)]. The adequacy of this method has been discussed in detail elsewhere.[30] Its main features are summarized here. The two branches of a symmetric hysteresis loop (i.e., one measured between opposite values of vertex field H_V) are linearly combined to get the half-sum Σ and half-difference Δ:

$$\Sigma = \frac{1}{2}[M_+(H) + M_-(H)],$$

$$\Delta = \frac{1}{2}[M_+(H) - M_-(H)]. \qquad (1)$$

The half-sum Σ has been proven to be exactly coincident with the anhysteretic magnetization curve,[30] which may be fitted to a superposition of Langevin functions.[3] Such a fitting procedure will be justified in Sec. IV C. In this way, the saturation magnetization M_s is obtained with a high degree of confidence, and the reduced half-sum m and half-difference Δ_R are derived:

$$m = \frac{1}{2}[m_+(H) + m_-(H)],$$

$$\Delta_R = \frac{1}{2}[m_+(H) - m_-(H)], \qquad (2)$$

where $m_{\pm} = M_{\pm}/M_s$. Δ_R may be plotted as a function of m, as in Fig. 1(b)]. The maximum value of the $\Delta_R(m)$ curve is

just the reduced remanence m_R. The new representation strongly amplifies the details of hysteresis loops: the spread in the experimental data, apparent in Fig. 1(b)], is almost undetectable when one observes the usual hysteresis loops [compare with Fig. 1(a)]. The following analysis will make use of the m, $\Delta_R(m)$ representation of hysteresis loops. The reduced remanence is a function of the amplitude of H_V, monotonically decreasing for $H_V \to 0$. This behavior is shown in Fig. 2, where m_R is plotted vs m_V (the reduced vertex magnetization, univocally related to H_V) for a set of selected systems. At high values of H_V ($m_V \to 1$), the $m_R(m_V)$ curves always reach a plateau, (m_R^{max}); in other words, the maximum separation between loop branches stops increasing. These loops will be referred to as *major loops*. In all studied systems, loops performed using $H_V \geq 5 \times 10^3$ Oe are major loops. Loops performed up to a vertex field smaller than 5×10^3 Oe will be referred to as *minor loops*.

III. THEORY OF MAGNETIC HYSTERESIS IN GRANULAR SYSTEMS

The theory is first developed for an assembly of magnetic particles having the same magnetic moment μ. In magnetic granular systems, the magnetic moments are distributed;[31] extension to a moment distribution being straightforward, the results will be reported towards the end of this section.

The reduced magnetization of such a model system, in the absence of interactions among moments, is simply

$$m = L\left(\frac{\mu H}{kT}\right), \qquad (3)$$

where L is the Langevin function, defined as $L(x) = \coth(x) - 1/x$, where $x = \mu H/kT$. In granular systems, magnetic interactions are of dipolar and, possibly, Ruderman-Kittel-Kasuya-Yosida (RKKY)-like type. Let us consider, for the moment, the effect of a pure dipolar interaction between any
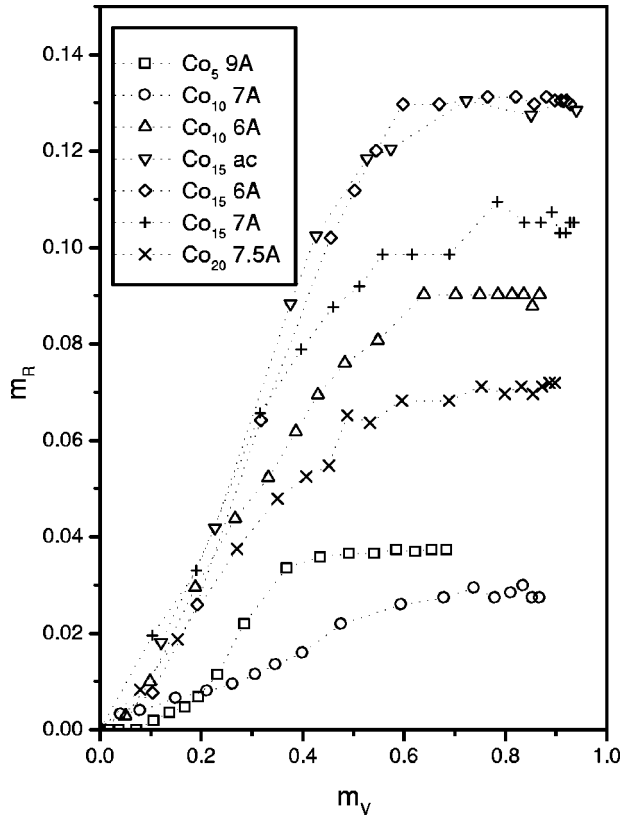
FIG. 2. Reduced remanence vs reduced vertex magnetization of minor loops for a set of selected $Cu_{100-x}Co_x$ samples.

two moments μ_i and μ_j at a distance r_{ij} apart. Such a choice will be shown later not to be particularly restrictive.

The interaction field of dipolar origin acting on site i is a random function of time, changing in magnitude, direction, and sign on a time scale whose characteristic time is the moment-moment relaxation time τ_2, which in these systems has been estimated to be of the order of a few tenths of a nanosecond ($\tau_2 \approx 2 \times 10^{-10}$ s).[32] The external field direction defining the z axis, the z component of the internal field of dipolar origin on the ith site is then

$$H_{iz}(t) = \sum_j A_{ij}\mu_{zj}(t) = \mu \sum_j A_{ij}u_j(t), \quad (4)$$

where $A_{ij} = (3cos^2\theta_{ij}-1)/r_{ij}^3$, θ_{ij} being the angle between the line connecting the ith and jth particles and the z axis, and where $u_j = \mu_{zj}/\mu$ is the cosine of the instantaneous angle between the direction of moment μ_j and the z axis. The time average of H_{iz} (performed over a time much larger than τ_2) is zero; similarly, the spatial average at fixed time of the random function H_{iz} over all magnetic sites is zero. In spite of this property, the presence of dipolar interactions significantly affects the equilibrium magnetization of the system, and its history under a varying external field. In fact, the characteristic time describing the approach to thermal equilibrium of the system of moments is the moment-lattice relaxation time τ_1, which in these systems and around room temperature has been estimated to be not much higher than τ_2 ($\tau_1 \approx 5 \times 10^{-10}$ s).[32] As a consequence, the dipolar interaction field is still effective in interfering with the thermal fluctuation of the ith moment, because it is not averaged out

during a typical fluctuation event. The local equilibrium state of the vector μ, although substantially determined by the values of absolute temperature and external field, is therefore affected to some extent by the dipolar field.

Our point is that this rather complex, statistical effect, which is presumed to be at the basis of magnetic hysteresis of these systems, may be accounted for in a comparatively simple way, i.e., by introducing in the argument of the Langevin function a properly defined ''memory function'' $\delta(m,m_V)$, depending on the actual magnetic state (m) and on the initial magnetic state (m_V) of the system. It is this term which ultimately gives rise to the hysteretic behavior for any given initial magnetization state (vertex magnetization) m_V. Specifically, the reduced magnetization on upper ($+$) and lower ($-$) branches of a hysteresis loop (that is, for decreasing and increasing magnetic field H, respectively) is

$$m_\pm = L\left(\frac{\mu H}{kT} \pm \delta(m_\pm,m_V)\right) \approx L\left(\frac{\mu H}{kT} \pm \delta(m,m_V)\right), \quad (5)$$

where the first expression indicates that, in principle, $m_\pm$ should be obtained by solving an implicit equation, while the second expression means that, to a good deal of approximation, the argument in the memory function may be substituted by the anhysteretic reduced magnetization, m.

In this view, the memory function indicates that any change in magnetic order is hindered by the weak magnetic interactions existing among magnetic-metal particles. In fact, the stability of the system against variations of any external parameter, such as the applied field, is slightly increased by the cumulative effect of magnetic interactions.

The *a priori* requirements for the memory function are the following:

(a) Eq. (5) must generate *closed* symmetric loops, i.e., the magnetization value after a complete symmetric loop ($+H_V \rightarrow -H_V \rightarrow +H_V$) must be coincident with the initial value;

(b) $\delta(m,m_V)$ must be larger where larger changes of m with H take place (this property makes the system of interacting moments similar, in a sense, to a continuous mechanical system characterized by an intrinsic viscosity);

(c) $\delta(m,m_V)$ must be an even function of m, reducing to zero for $H \rightarrow \pm\infty$ and $m \rightarrow \pm 1$ (i.e., the memory term must disappear when all moments are aligned).

Requirement (a) is fulfilled assuming that $\delta(m,m_V)$ is in the form of a difference:

$$\delta(m,m_V) = \delta(m) - \delta(m_V), \quad |m| < |m_V|, \quad (6)$$

where $\delta(m)$ is factorized as follows:

$$\delta(m) = 3\frac{dm}{dH}\Phi(m) \quad (7)$$

in order to satisfy requirement (b). Here dm/dH is the first derivative of the reduced magnetization with respect to H, an even function of H (and of m), while $\Phi(m)$ is another even function of m having the physical dimensions of a magnetic field, and describing the effect of the dipolar interaction. The factor of 3 appearing in the δ function [Eq. (7)] has been explicitly added in view of the subsequent introduction of a new quantity, which will play a central role in the theory [see

below, Eq. (11), and related text]. Note that $3dm/dH = 3u'\mu/kT$, where u' is the first derivative of the Langevin function $L(x)$ with respect to its argument, so that when $H = 0$, $3dm/dH = 3u'(0)\mu/kT = \mu/kT$. Basically, $\Phi(m)$ is defined as the root-mean-square value of the random field H_{zi}:

$$\Phi(m) \equiv \langle H_{zi}^2 \rangle^{1/2} = \left(\sum_{jk} A_{ij}A_{ik}\langle u_j u_k \rangle \right)^{1/2}, \qquad (8)$$

which may be written as (see the Appendix):

$$\Phi(m) = \sqrt{3}\tilde{H}_o(\langle u^2 \rangle - \langle u \rangle^2)^{1/2}$$
$$\equiv \sqrt{3}\tilde{H}_o(\langle u^2 \rangle - m^2)^{1/2}, \qquad (9)$$

$\langle u^2 \rangle$ being the second moment of u_j, which corresponds to

$$\langle u^2 \rangle = 1 - \frac{2L\left(\dfrac{\mu H}{kT}\right)}{\dfrac{\mu H}{kT}} \qquad (10)$$

and $\tilde{H}_o = \mu(\frac{1}{3}\Sigma_j A_{ij}^2)^{1/2} \equiv (1/\sqrt{3})H_i$, where H_i is an effective interaction field, already estimated to be of the order 200–1000 Oe in the $Cu_{100-x}Co_x$ system.[32] The function $\Phi(m)$ takes its maximum value ($\tilde{H}_o$) for $m=0$, and reduces to zero as $(1-|m|)^2$ for $m \rightarrow \pm 1$. Requirement (c) is naturally satisfied by $\Phi(m)$ and a fortiori by $\delta(m)$. The decrease of $\Phi(m) \equiv \langle H_{zi}^2 \rangle^{1/2}$ with m has a simple physical explanation: in fact, when all moments become parallel, the dipolar field on any site is identically zero, provided it originates from an assembly of equal moments randomly distributed in space, as we are assuming here [33]. The memory function is finally written as

$$\delta(m,m_V) = 3\sqrt{3}\frac{\mu\tilde{H}_o}{kT}\{u'(\langle u^2 \rangle - m^2)^{1/2}$$
$$- u'_V(\langle u^2 \rangle_V - m_V^2)^{1/2}\}$$
$$= \frac{\mu\tilde{H}_o}{kT}[F(m) - F(m_V)], \qquad (11)$$

where $F(m) = 3\sqrt{3}u'(\langle u^2 \rangle - m^2)^{1/2}$ is a monotonically decreasing, even function of m. The factor $3\sqrt{3}$ causes $F(m)$ to range between the limits $F(0)=1$, $F(1)=0$. $F(m)$ will be referred to in the following as the ''cutoff'' function, because it represents how the memory function is attenuated by increasing the alignment of magnetic moments, owing to the decrease of the rms dipolar field. The factor $\mu\tilde{H}_o/kT$ is a small quantity at room temperature, being of the order of 0.12 for parameter values appropriate to this case ($\mu = 5 \times 10^{-17}$emu and $\tilde{H}_o = 1 \times 10^2$ Oe). Note that in this way the effect of dipolar interaction has been cast in the form of a mean field, H_{mean}:

$$m_\pm = L\left(\frac{\mu}{kT}(H \pm H_{mean})\right), \qquad (12)$$

where $H_{mean} \equiv \tilde{H}_o[F(m) - F(m_V)]$ is however a *decreasing* function of m, and has a sign depending on the one of $d|m|/dH$. The emergence of a mean-field theory is fully compatible with the long-range character of the dipolar interaction.[34] The whole theory may be checked on actual $Cu_{100-x}Co_x$ systems. It is worth noting that the only adjustable parameter of the model is the value of $\tilde{H}_o$, all other terms being known or obtained from the experiment.

IV. APPLICATION OF THE THEORY

The main predictions of the model are summarized here.

A. Dependence of remanence on vertex field

The value of the positive reduced remanence is

$$m_R(m_V) = L\left(\frac{\mu\tilde{H}_o}{kT}[1 - F(m_V)]\right) \cong \frac{1}{3}\frac{\mu\tilde{H}_o}{kT}[1 - F(m_V)]. \qquad (13)$$

One can observe that m_R is a function of the loop's vertex field through the vertex magnetization value. For a major loop, m_V approaches unity and $F(m_V)$ approaches zero, so that m_R reaches its maximum value

$$m_R^{max} = L\left(\frac{\mu\tilde{H}_o}{kT}\right) \cong \frac{1}{3}\frac{\mu\tilde{H}_o}{kT}. \qquad (14)$$

For minor symmetric loops, m_R is predicted to decrease with decreasing H_V or m_V: see Fig. 2. The reduced remanence of a major loop is therefore a measure of the intensity of the field $\tilde{H}_o$, at least in the high-temperature limit. Equation (14) provides a way to easily determine $\tilde{H}_o$ from experimental data.

B. Dependence on reduced magnetization of reduced half-difference of loop branches

The half-difference between upper and lower branches of a reduced loop, developed to the first order in the small parameter $\mu H_{mean}/kT$, takes the form:

$$\Delta_R(m) \cong \frac{\mu\tilde{H}_o}{kT}[F(m) - F(m_V)]u'(m). \qquad (15)$$

For a major loop, $F(m_V) \cong 0$, therefore

$$\Delta_R(m) \cong \frac{\mu\tilde{H}_o}{kT}F(m)u'(m). \qquad (16)$$

C. Anhysteretic curve

Whereas the reduced half-difference is proportional to the small parameter $\mu H_{mean}/kT$, the reduced half-sum (i.e., the anhysteretic magnetization curve) is nearly coincident with the Langevin function for noninteracting moments [Eq. (3)], because in this case the dipolar interaction merely introduces a second-order correction:

$$m \cong L\left(\frac{\mu H}{kT}\right) + \frac{1}{2}\left(\frac{\mu H_{mean}}{kT}\right)^2 u''\left(\frac{\mu H}{kT}\right) \cong L\left(\frac{\mu H}{kT}\right). \qquad (17)$$

The anhysteretic curve therefore closely represents the magnetization behavior of the granular system where the interaction among particles has been turned off. This circumstance implies that the magnetic-moment values obtained by fitting the anhysteretic curve to a superposition of Langevin functions are essentially correct, even in interacting systems.

D. Self-consistency of the theory

A proof of the validity of this theory may be obtained by considering the two independent ways of experimentally determining the cutoff function by means of Eqs. (13), (14), and (16). In fact, exploiting Eq. (13) $F(m_V)$ may be canonically determined in terms of the vertex magnetization of a complete set of minor symmetrical loops, as

$$F(m_V) = 1 - \frac{m_R(m_V)}{m_R^{\max}}, \tag{18}$$

where all quantities in the right-hand side are experimentally determined (Fig. 2). On the other hand, using Eq. (16) the cutoff function may be independently obtained from a single major loop:

$$F(m) = \frac{\Delta(m)}{3 m_R^{\max} \cdot u'(m)}, \tag{19}$$

where again all quantities in the right-hand side are known from experiment. In principle, the first method is far more accurate than the second one, because the denominator in the fraction of Eq. (19) approaches zero (as the numerator does) for $m \to \pm 1$, inducing large fluctuations in the values of $F(m)$. However, the second method involves a single measurement of a major loop, and is much faster. In any case, Eqs. (18) and (19) provide two independent ways of obtaining the same function; the results for $F(m)$ and $F(m_V)$ may be plotted together on the same horizontal scale, as shown in Fig. 3. The agreement between the two data sets is striking in all examined cases, and provides a strong clue about the validity of the whole theory.

E. Form of the theory for distributed moments. Validity of the model

A further step consists in extending Eq. (12) to a real system, where the moments are distributed in size. Let p_n be the fraction of magnetic moments of magnitude μ_n; the expressions for the reduced anhysteretic magnetization and for the branches of a hysteresis loop are simply

$$m = \sum_n p_n L\left(\frac{\mu_n H}{kT}\right) \tag{20}$$

and

$$m_\pm = \sum_n p_n L\left(\frac{\mu_n}{kT}(H \pm H_{\mathrm{mean}})\right), \tag{21}$$

where H_{mean} is defined as before, but using the average value μ_o of the magnetic moments in the expression for $F(m)$:

$$\mu_o = \sum_n p_n \mu_n,$$

$$m_o = L\left(\frac{\mu_o H}{kT}\right),$$

$$\langle u^2 \rangle_o = \frac{1 - 2L\left(\dfrac{\mu_o H}{kT}\right)}{\dfrac{\mu_o H}{kT}},$$

$$u'_o \equiv L'\left(\frac{\mu_o H}{kT}\right),$$

$$F_o(m) \equiv F(m_o) = 3\sqrt{3} u'_o [\langle u^2 \rangle_o - m_o^2]^{1/2}, \tag{22}$$

where the quantities in the right-hand term of the last line are evaluated for the same field value at which the value m of the abscissa is calculated according to Eq. (20). The agreement between theory and experiment is shown in Fig. 4 for all examined systems. The symbols always refer to the cutoff function experimentally obtained by applying Eq. (19); the lines are the corresponding theoretical predictions for pure dipolar interaction. Two main features may be evidenced:

(a) the agreement between experimental and theoretical $F(m)$ curves is very good for low Co content ($x = 5$, 10 at. %), becoming increasingly worse for $x > 10$ at. %, when the experimental cutoff function appears to be sharper than predicted around $m = 0$. In any case, for $x = 5, 10$, 15 at. % the overall behavior of all $F(m)$ curves—and consequently of hysteresis loops—is accurately described by a theory considering superparamagnetic particles and dipolar interactions only. This result may indicate that, at least for low Co content, other possible interactions are weaker than dipolar coupling. This evidence is in complete agreement with recent Monte Carlo simulation results, indicating that the dipolar term is much stronger than the indirect RKKY term, owing to the intrinsic oscillatory nature of the latter.[35] At higher Co concentration, either additional interaction mechanism begins to play a role, or the blocked-particle effects become no longer negligible, even at room temperature;

(b) all cutoff functions belonging to the same family are practically coincident, both experimentally and theoretically [the actual differences among theoretical curves essentially depend on values of μ_o only slightly varied from sample to sample, and are always very small; they are consequently shown in just one case, see Fig. 4(b)]. Once again, no free parameters were used in producing the theoretical curves in Figs. 4.

F. Major symmetric loops

The adequacy of the theory to fit the whole hysteretic magnetization curves of $\mathrm{Cu}_{100-x}\mathrm{Co}_x$ granular systems is pointed out in Fig. 5, where selected experimental and theoretical loops, both major and minor, are plotted together. The agreement between theory and experiment is always as good as the one shown in Fig. 5, where not all collected experimental data (symbols) are actually displayed, in order to deal with more readable plots. Note that the theoretical loops cor-
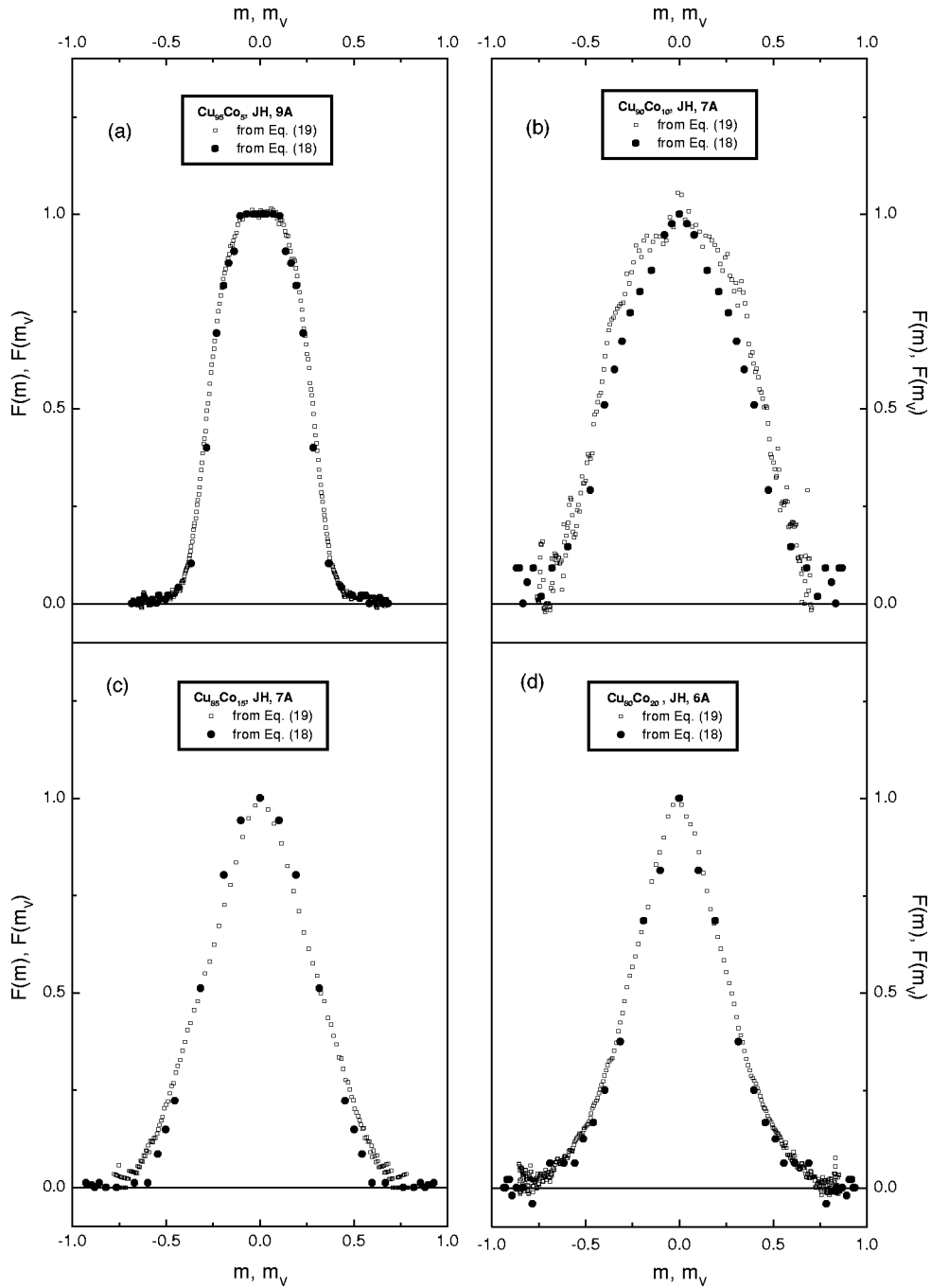
FIG. 3. Cutoff function obtained from a single major loop (open symbols) and from different minor loops (full symbols) for samples of $Cu_{95}Co_5$ (a), $Cu_{90}Co_{10}$ (b), $Cu_{85}Co_{15}$ (c), and $Cu_{80}Co_{20}$ (d).

rectly close at both vertexes, owing to the form of the $\delta(m,m_V)$ function. These loops were obtained as follows: first, the anhysteretic curve was measured; then, it was fitted to a superposition of a few Langevin functions. In this way, both the average moment μ_o and the saturation magnetization were obtained, and the $F_o(m)$ function was generated. The field $\tilde{H}_o$ was determined by fitting the experimental reduced remanence of major loops [Eq. (14)]. Finally, the loop branches were generated using Eq. (21). In the present case, only two Langevin functions, corresponding to two different magnetic-moment values, were used. This is of course a somewhat crude representation of the actual distribution of magnetic moments in such granular systems; however, such

a choice has been made (here as well as in Refs. 3 and 34) because increasing the number of discrete moment values, or even introducing a continuous distribution of moments, expressed by a function $p(\mu)$, brings about a relatively insignificant increase in the precision of the fit, at the cost of heavily reducing the reliability of the obtained fitting parameters.

G. Minor symmetric loops: Remanence-coercivity relationship

A closely linear relation between reduced remanence and coercivity, similar to the one discussed in Ref. 34, also holds for minor loops. In fact, indicating the coercivity of a loop
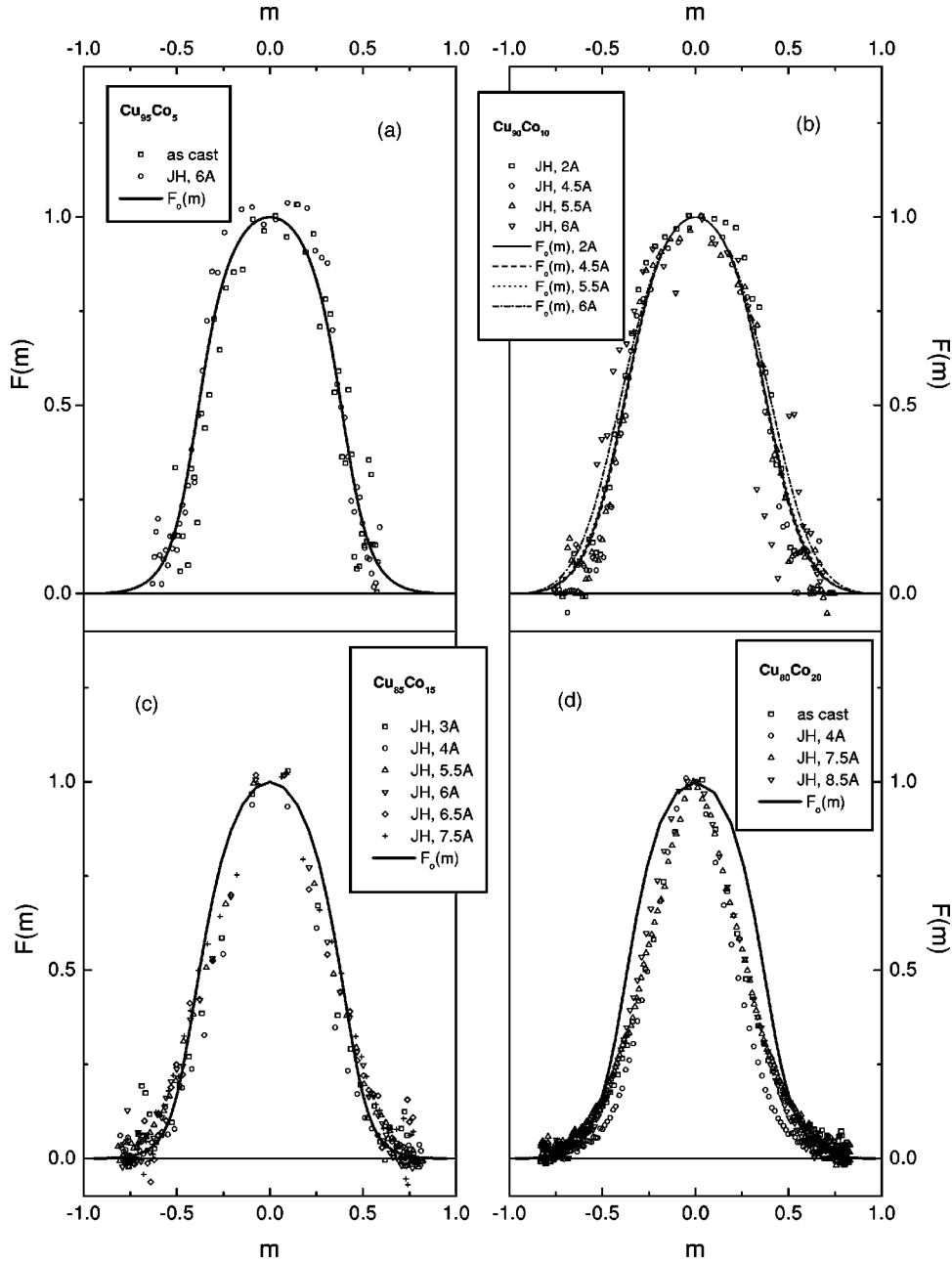
FIG. 4. Experimental cutoff functions and theoretical predictions for different $Cu_{95}Co_5$ (a), $Cu_{90}Co_{10}$ (b), $Cu_{85}Co_{15}$ (c), and $Cu_{80}Co_{20}$ (d) samples. The differences among theoretical curves, always very small, are reported only for case b.

with vertex field H_V as H_{cV}, and $m_R(m_V)$ given by Eq. (13) as m_{RV}, the following formula is obtained by manipulating Eqs. (13) and (22) to the second order in the small parameter ($\mu_o H_{cV}/3kT$):

$$m_{RV} = \frac{\mu_o H_{cV}}{3kT} + \frac{27}{5} m_R^{max} \left(\frac{\mu_o H_{cV}}{3kT} \right)^2, \qquad (23)$$

where m_R^{max} is the reduced remanence of a major loop (see Fig. 2) and μ_o is the average magnetic moment [Eq. (22)]. The agreement between theory (lines) and experiment (symbols) is shown in Fig. 6 and turns out to be rather good for all examined systems. Note that all theoretical lines are almost coincident, and that the quadratic term only provides a small correction to the linear law.

H. Minor asymmetric loops: Demagnetizing a granular system

The theory may also be used to predict the magnetization behavior in asymmetric loops, like the ones observed during a demagnetization procedure. In such a case, the vertex field values form a sequence of the type: $+H_{V0}$, $-H_{V1}$, $+H_{V2}$, $-H_{V3}$, ... , where $|H_{V,n+1}| < |H_{V,n}|$. We have chosen a demagnetizing procedure characterized by the law

$$|H_{V,n+1}| = \frac{1}{2} |H_{V,n}|, \qquad (24)$$

starting with $H_{V,0} = +1 \times 10^4$ Oe and ending with $H_{V,6} = +156$ Oe. The complete field history of the magnetization of a selected sample ($Cu_{90}Co_{10}$, JH, $I = 7A$) is shown in Fig. 7(a); the central region is expanded in Fig. 7(b) to evidence the three descending (odd) branches and the three ascending (even) ones. The corresponding remanence values (both positive and negative) are well determined from these curves; they are reported (as reduced values) in Fig. 7(c) as functions of the branch number (full symbols).
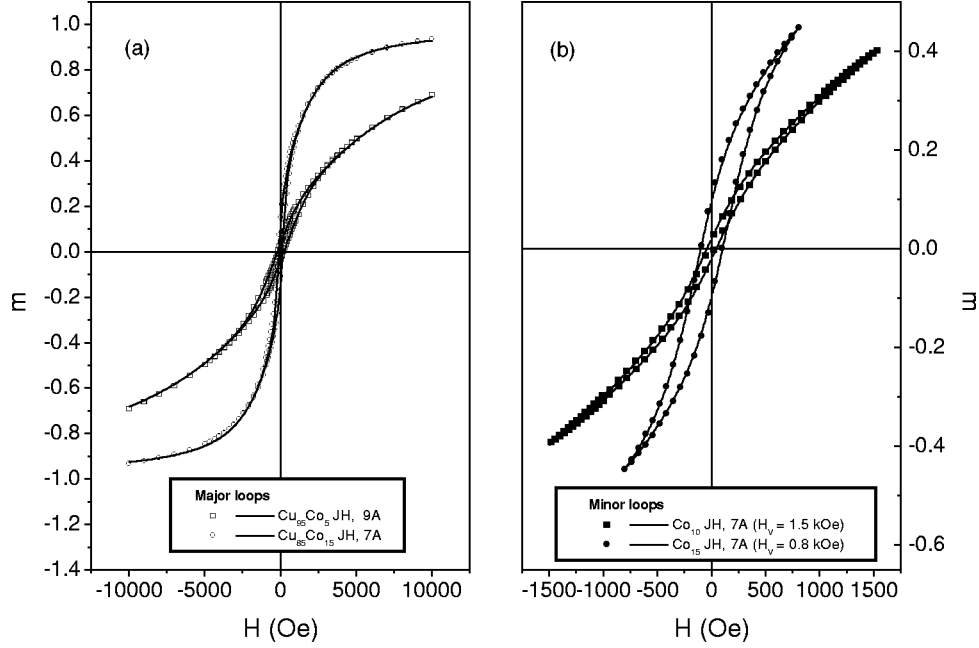
FIG. 5. Major (a) and minor (b) loops of selected samples of $Cu_{95}Co_5$, $Cu_{90}Co_{10}$, $Cu_{85}Co_{15}$. Symbols: experimental data; lines: theory.

In this case, the theory predicts that the δ function for subsequent loop branches must keep the memory of all previous vertex magnetization values, according to the following scheme:

First branch (descending):

$$\delta = \delta(m, m_{V0}) = \frac{\mu \tilde{H}_o}{kT}[F(m) - F(m_{V0})].$$

Second branch (ascending):

$$\delta(m, m_{V0}, m_{V1}) = \frac{\mu \tilde{H}_o}{kT}[F(m) - 2F(m_{V1}) + F(m_{V0})].$$
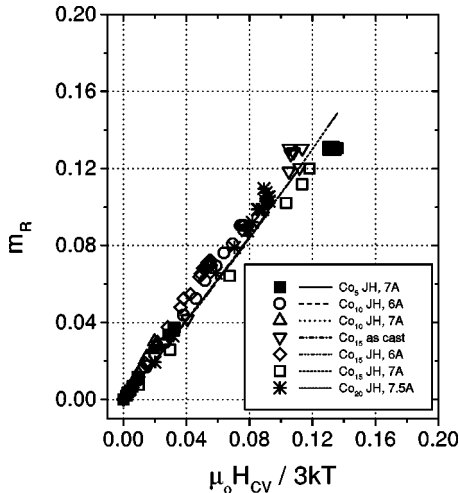
Third branch (descending):

FIG. 6. Reduced remanence vs $\mu_o H_{cV}/3kT$ (μ_o is the average magnetic moment; H_{cV} is the vertex field; T is the room temperature) for different samples of $Cu_{100-x}Co_x$. Lines indicate the theory. Note that all lines are almost coincidental.

$$\delta = \delta(m, m_{V0}, m_{V1}, m_{V2}) = \frac{\mu \tilde{H}_o}{kT}[F(m) - 2F(m_{V1})$$
$$+ 2F(m_{V2}) - F(m_{V0})],$$

and so on. In this way, the continuity of magnetization branches at all vertexes is automatically guaranteed. The magnetization values on the first three branches are, in fact,

$$m_+^{(1)} = L\left(\frac{\mu H}{kT} + \frac{\mu \tilde{H}_o}{kT}[F(m) - F(m_{V0})]\right),$$

$$m_-^{(2)} = L\left(\frac{\mu H}{kT} - \frac{\mu \tilde{H}_o}{kT}[F(m) - 2F(m_{V1}) + F(m_{V0})]\right),$$

$$m_+^{(3)} = L\left(\frac{\mu H}{kT} + \frac{\mu \tilde{H}_o}{kT}[F(m) - 2F(m_{V1}) + 2F(m_{V2})\right.$$
$$\left. - F(m_{V0})]\right),$$

and so on. One can easily check that $m_+^{(1)}(H = -H_{V1}) \equiv m_-^{(2)}(H = -H_{V1})$, as well as for all considered vertexes. The sequence of reduced remanence values is, therefore,

$$m_R^{(1)} \cong \frac{1}{3} \frac{\mu \tilde{H}_o}{kT}[1 - F(m_{V0})] \cong m_R^{max},$$

$$m_R^{(2)} \cong -m_R^{max}[1 - 2F(m_{V1})],$$

$$m_R^{(3)} \cong +m_R^{max}[1 - 2F(m_{V1}) + 2F(m_{V2})],$$

the general term being

$$m_R^{(n)} \cong (-1)^{n-1} m_R^{max}[1 - 2F(m_{V1}) + \cdots$$
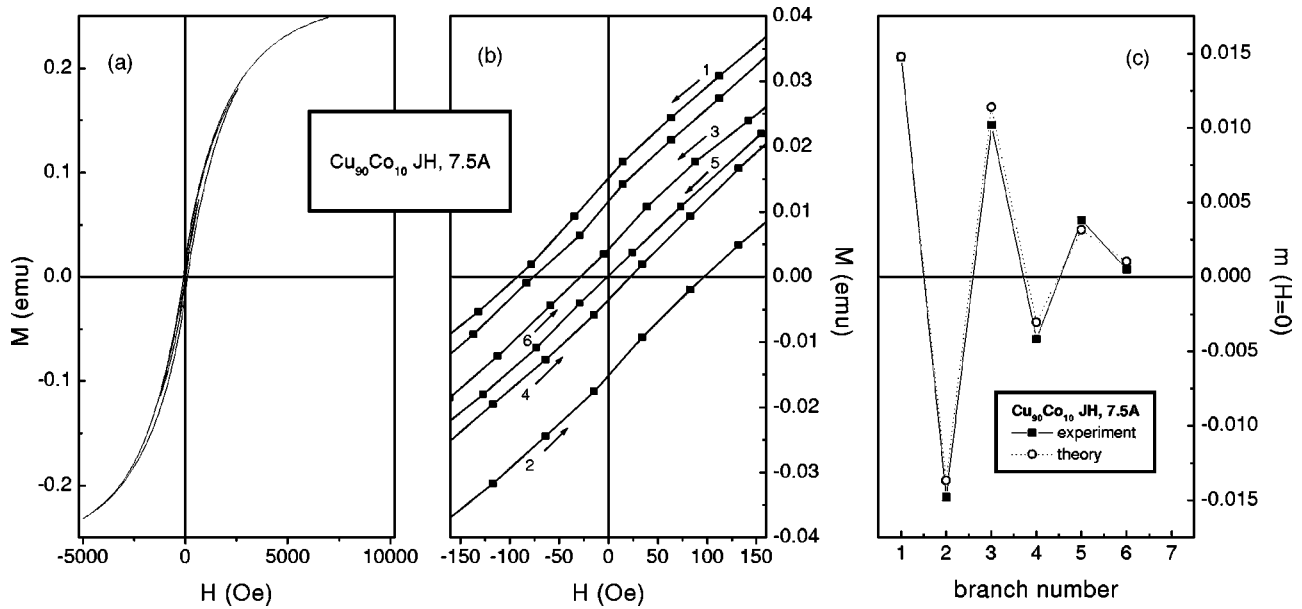$$+ (-1)^{n-1} 2F(m_{V,n-1})].$$

FIG. 7. Complete demagnetization history of a joule-heated $Cu_{90}Co_{10}$ sample; (a) overall magnetization behavior; (b) detail around $H=0$ (branch numbers are indicated); (c) experimental values of the reduced remanence (from b; full symbols) and model's prediction (open symbols) as functions of branch number.

These values are reported in Fig. 7(c) (open circles). Once again, the agreement between theory and experiment is very good.

It is interesting to remark that both theory and experiment clearly indicate that in the examined case a truly demagnetized state ($m_R=0$) is not reached, although the final value of m_R is close to zero. This result is related to the specific choice of the demagnetization procedure, which occurs in a few steps, each vertex field being halved with respect to the previous one. The condition $m_R=0$ is actually reached when the demagnetization procedure involves a much larger number of steps, of the order of several tens (in such a case, each vertex field in the sequence is only slightly lower than the previous one). For just a few steps with big vertex-field jumps, the final value of m_R may be either small and positive (as in the present case) or small and negative.

I. Reference states: First magnetization curve

At both low and intermediate fields ($H \lesssim 5 \times 10^3$ Oe), the field history of magnetization may become very complex by effect of the peculiar behavior of the function δ which keeps the memory of all previous vertex-magnetization values, as already evidenced in the description of asymmetric minor loops. As a consequence, the magnetization is not a single-valued function of the external field. In principle, a one-to-one correspondence between H and m only occurs in the limit $|H| \to \infty, |m| \to 1$, i.e., when all moments are aligned and the magnetic entropy of the system is zero. In practice, however, such a one-to-one correspondence occurs when the $\delta(m)$ function given by Eq. (11) becomes negliglible with respect to $\mu H/kT$, which is the leading term in Eq. (5). The loop's branches then merge, within the experimental uncertainty, into a single Langevin curve [Eq. (3)], and the magnetization behavior becomes fully anhysteretic. The memory function may be considered negligible when $F(m) \to 0$ [Eq. (11) and Fig. 3], quite independently of the previous field

history. Fig. 3 clearly indicates that in all examined cases $F(m) \approx 0$ when $m \approx 0.75$ (such a value is reached for $H=H^* \approx 5 \times 10^3$ Oe for $x=5$, 10 at. %, and for $H=H^* \approx 1 \times 10^3$ Oe for $x=15,20$ at. %). Any magnetic state corresponding to an applied field larger than H^* is described by a single-valued magnetization, and may be considered as a good reference state, i.e., a magnetic state independent of the previous field history. On the contrary, the states at $H=0$ and $m \approx 0$ do not fulfill such a condition.

To further illustrate this point, let us briefly comment on the so-called first magnetization curve of any of our samples. Such a curve starts from the state ($H=0$, $m=0$), which is only reached by performing a complete demagnetization procedure of the type discussed in the previous subsection. When H is again increased, starting from zero, the reduced magnetization on the resulting curve (m_{first}) is described by the equation:

$$m_{first} = L\left(\frac{\mu H}{kT} - \frac{\mu \widetilde{H}_o}{kT}[F(m) - S] \right), \qquad (25)$$

where S represents the total contribution of all terms in the memory function arising from the demagnetizing procedure followed. It is easily recognized that $S=1$ if the requirement $m_{first}(H=0)=0$ has to be satisfied. As a consequence, m_{first} can be written as

$$m_{first} = L\left(\frac{\mu H}{kT} + \frac{\mu \widetilde{H}_o}{kT}[1 - F(m)] \right). \qquad (26)$$

The term $1 - F(m)$ is very close to zero when $H \lesssim \widetilde{H}_o$, while it approaches unity when $H \approx H^* \gg \widetilde{H}_o$. The relative difference $\Delta m/m = (m_{first} - m)/m$, where m is the anhysteretic magnetization given by the Langevin function [Eq. (3)], is

$$\frac{\Delta m}{m} = \frac{\mu \tilde{H}_o}{kT} \frac{[1 - F(m)]u'}{m}, \tag{27}$$

taking its maximum value for $m \approx 0.4$. It is easily checked that $\Delta m/m$ never exceeds 3%, so that the first magnetization curve is almost coincident with the anhysteretic Langevin function.

V. CONCLUDING REMARKS

The proposed theory successfully explains in detail all the examined features of hysteresis loops observed in the $Cu_{100-x}Co_x$ system. This is, to our knowledge, one of the very rare cases where an analytical theory of magnetic hysteresis has been set out, the most fruitful approach being usually a statistical one.[37] The intrinsic coherence of the theory has been discussed in Sec. IV D. However, another type of coherence is remarkable: in fact, the *same* set of magnetic-moment values and weights needed to fit the anhysteretic magnetization curve is used to fit all properties of the hysteresis loop. Moreover, the *same* set may also be used to describe the giant magnetoresistance behavior of the system in the framework of Ref. 3.

A central role in this mean-field theory is played by the memory function $\delta(m)$, which contains both the function $\Phi(m)$ (taking into account the cumulative effect of dipolar interaction) and the derivative term dm/dH. Actually, any function of the type $f(dm/dH)$ could, in principle, appear in Eq. (7); however, the agreement between theory and experiment indicates that the simple representation of $\delta(m)$ given by Eq. (7) is substantially correct.

The effective interaction field H_i is not obtained from first principles [the field $\tilde{H}_o$ appearing in Eq. (9) is just $H_i/\sqrt{3}$]. As a matter of fact, all the values of $\tilde{H}_o$ arising from the experimental reduced remanences through Eq. (14) lie between 80 and 300 Oe, in agreement with the estimated H_i values (200–1000 Oe).[32] However, the values of H_i for a given sample are not exactly predictable on the basis of the known structural data (average particle size, average interparticle distance) for that sample. This may be considered as an intrinsic limit of the proposed approach.

In real systems, a broad distribution of magnetic-moment values can be present, as evidenced in a few cases by actual particle observation,[8,36] so that magnetic contributions from both superparamagnetic and blocked particles can be expected. As a matter of fact, magnetization curves of granular systems are often explained in terms of a mere superposition of independent effects of this type. Although such a picture cannot be excluded, we point out here the relevant role played in granular systems by interparticle, rather than single-particle, effects. It should be stressed that in any granular system the present theory becomes applicable only in the high-temperature limit, where blocked-particle effects are negligible.

In other approaches, the presence of weak interactions among fine magnetic particles is taken into account by introducing an additional term to the energy barrier overcome by the particle magnetization in a spin-flip process.[4,25] In this way, a genuine interparticle effect is again described within the framework of a single-particle picture. We have followed another way of representing magnetic interactions, possibly less simple, but more suitable to describe magnetic hysteresis.

Our analysis suggests that the dominant interaction among magnetic moments is of a dipolar nature, at least for low Co content. In fact, dipolar interaction is sufficient to accurately describe and predict all the details of hysteretic magnetization.

The effect of these weak, long-ranged interactions has been described by a sort of mean-field theory (where however the mean field *decreases* with m, instead of being a linear function of m). Using a mean-field approach implies completely neglecting the correlation among individual magnetic moments, which are considered to be statistically independent. Such a simplifying assumption is, however, justified in an analysis dealing with thermal-equilibrium properties of the system of moments, i.e., with properties investigated through experiments involving measurement times much larger than τ_1. As known, magnetic correlations play instead a significant role in determining the giant magnetoresistance behavior of $Cu_{100-x}Co_x$ systems.[3] In fact, the latter effect essentially results from spin-dependent scattering of conduction electrons by adjacent magnetic moments; in that case, the electrons explore a nearly instantaneous, off-equilibrium local magnetic state (the electronic time-of-flight between adjacent magnetic particles being much shorter than τ_1 at room temperature[32]). The following hierarchy may therefore be established when different physical properties of granular systems are studied: (a) the anhysteretic magnetization is well described in terms of a pure Langevin function, i.e., neglecting the existence of both magnetic interactions and correlations among magnetic moments; (b) the hysteresis loop can be described in terms of a mean-field term added to the argument of the Langevin function, i.e., taking into account dipolar interactions, but still neglecting magnetic correlations; (c) the magnetoresistance can be described by a more complex approach, explicitly considering the effect of instantaneous magnetic correlations among interacting magnetic moments.

Finally, it should be noted that the theory, although rather complete, has been checked only at room temperature. The next step will consist in applying the model to describe hysteretic features at both lower and higher temperatures, where spurious effects, respectively, related to the progressive blocking of superparamagnetic particles, and to possible changes in particle number and size, will have to be properly taken into account. Moreover, the theory will have to be tested on different magnetic systems containing ultrafine particles, in order to establish the domain of its prospective application.

ACKNOWLEDGMENTS

APPENDIX

The time-dependent dipolar field acting on the ith site is given by Eq. (4). When all magnetic moments are aligned ($u_j = 1$) and are randomly distributed in space, H_{iz} is identically zero[33]

$$\sum_j A_{ij}=0. \tag{A1}$$

The square of the instantaneous dipolar field on site i is

$$H_{iz}^2=\mu^2\sum_j \sum_k A_{ij}A_{ik}u_ju_k. \tag{A2}$$

The average value of H_{iz}^2 is

$$\langle H_{iz}^2\rangle=\mu^2\sum_j \sum_k A_{ij}A_{ik}\langle u_ju_k\rangle. \tag{A3}$$

Time average (over times larger than τ_2) and space average (over all sites i) of H_{iz}^2 are considered to be coincident. For uncorrelated magnetic moments, the pair-correlation function $\langle u_ju_k\rangle$ takes the form:

$$\langle u_ju_k\rangle=\langle u^2\rangle(j=k),$$

$$\langle u_ju_k\rangle=\langle u\rangle^2=m^2(j\neq k), \tag{A4}$$

so that

$$\langle H_{iz}^2\rangle=\mu^2\sum_j A_{ij}^2\langle u^2\rangle+\mu^2\sum_j \sum_{k\neq j} A_{ij}A_{ik}m^2. \tag{A5}$$

Using Eq. (A1), one gets

$$\sum_j \sum_{k\neq j} A_{ij}A_{ik}=-\sum_j A_{ij}^2, \tag{A6}$$

and finally

$$\langle H_{iz}^2\rangle=\mu^2\left(\sum_j A_{ij}^2\right)[\langle u^2\rangle-m^2]=3\tilde{H}_o^2[\langle u^2\rangle-m^2]. \tag{A7}$$

See Eq. (9).

---

[1] *Science and Technology of Nanostructured Magnetic Materials*, Vol. 259 of *NATO Advanced Study Institute, Series B: Physics*, edited by G. C. Hadjipanayis and G. A. Prinz (Plenum, New York, 1991).

[2] *Magnetic Properties of Fine Particles*, edited by J. L. Dormann and D. Fiorani (North-Holland, Amsterdam, 1992).

[3] P. Allia, M. Knobel, P. Tiberto, and F. Vinai, Phys. Rev. B **52**, 15 398 (1995).

[4] S. Morup and E. Tronc, Phys. Rev. Lett. **72**, 3278 (1994).

[5] J. Garcia-Otero, A. J. Garcia-Bastida, and J. Rivas, J. Magn. Magn. Mater. **189**, 377 (1998).

[6] C. L. Chien, J. Appl. Phys. **69**, 5267 (1991).

[7] A. Hütten and G. Thomas, Ultramicroscopy **52**, 581 (1993).

[8] A. Lopez, F. J. Lazaro, R. Von Helmolt, J. L. Garcia-Palacios, J. Wecker, and H. Cerva, J. Magn. Magn. Mater. **187**, 221 (1998).

[9] J. L. Dormann, R. Cherkaoui, L. Spinu, M. Nogus, F. Lucari, F. D'Orazio, D. Fiorani, A. Garcia, E. Tronc, and J. P. Jolivet, J. Magn. Magn. Mater. **187**, L139 (1998).

[10] J. R. Childress and C. L. Chien, Phys. Rev. B **43**, 8089 (1991).

[11] A. E. Berkowitz, J. R. Mitchell, M. J. Carey, A. P. Young, S. Zhang, F.E. Spada, F. T. Parker, A. Hütten, and G. Thomas, Phys. Rev. Lett. **68**, 3745 (1992); J. Q. Xiao, J. S. Jiang, and C. L. Chien, *ibid.* **68**, 3749 (1992).

[12] S. Mitani, H. Fujimori, and S. Ohnuma, J. Magn. Magn. Mater. **177-181**, 919 (1998).

[13] A. B. Pakhomov, X. Yan, and Y. Xu, Appl. Phys. Lett. **67**, 3497 (1995).

[14] C. P. Bean and J. D. Livingston, J. Appl. Phys. **30**, 120 (1959).

[15] E. C. Stoner and E. P. Wohlfarth, Philos. Trans. R. Soc. London, Ser. A **240**, 599 (1948); reprinted by IEEE Trans. Magn. **27** (4), 3475 (1991).

[16] D. A. Dimitrov and G. M. Wysin, Phys. Rev. B **54**, 9237 (1996).

[17] M. El Ghannami, C. Gomez-Polo, G. Rivero, and A. Hernando, Europhys. Lett. **26**, 701 (1994).

[18] J. L. Dormann, F. D'Orazio, F. Lucari, E. Tronc, P. Prené, J. P. Jolivet, D. Fiorani, R. Cherkaoui, and M. Nogués, Phys. Rev. B **53**, 14 291 (1996).

[19] M. El-Hilo, R. W. Chantrell, and K. O'Grady, J. Appl. Phys. **84**, 5114 (1998).

[20] G. Szabó and G. Kádár, Phys. Rev. B **58**, 5584 (1998).

[21] D. Kechrakos and K. N. Trohidou, Phys. Rev. B **58**, 12 169 (1998).

[22] J. M. González, O. A. Chubykalo, and J. Gonzáles, Phys. Rev. B **55**, 921 (1997).

[23] M. Knobel, E. F. Ferrari, and F. C. S. da Silva, Mater. Sci. Forum **302-303**, 169 (1999).

[24] R. Iglesias, H. Rubio, and S. Suárez, Appl. Phys. Lett. **73**, 2503 (1998).

[25] J. L. Dormann, D. Fiorani, and E. Tronc, Adv. Chem. Phys. **98**, 283 (1997).

[26] A. Hernando and T. Kulik, Phys. Rev. B **49**, 7064 (1994).

[27] A. Slawska-Waniewska, P. Nowicki, H. K. Lachowicz, P. Gorria, J. M. Barandiarán, and A. Hernando, Phys. Rev. B **50**, 6465 (1994); A. Slawska-Waniewska and J. M. Greneche, *ibid.* **56**, R8491 (1997).

[28] R. W. McCallum, A. M. Kadin, G. B. Clemente, and J. E. Keem, J. Appl. Phys. **61**, 3577 (1987); E. F. Kneller and R. Hawing, IEEE Trans. Magn. **27**, 3588 (1981).

[29] P. Allia, M. Baricco, P. Tiberto, and F. Vinai, Rev. Sci. Instrum. **64**, 1053 (1993).

[30] P. Allia, M. Coisson, P. Tiberto, and F. Vinai (unpublished).

[31] P. Allia, F. Ghigo, M. Knobel, P. Tiberto, and F. Vinai, J. Magn. Magn. Mater. **157-158**, 319 (1996).

[32] P. Allia, P. Tiberto, and F. Vinai, J. Appl. Phys. **81**, 4599 (1997).

[33] See, e.g., N. W. Ashcroft and N. D. Mermin, *Solid State Physics* (Saunders College, Philadelphia, 1988), p. 541.

[34] P. Allia, M. Coisson, M. Knobel, P. Tiberto, and F. Vinai, J. Appl. Phys. **85**, 4343 (1999).

[35] D. Altbir, J. D'Albuquerque e Castro, and P. Vargas, Phys. Rev. B **54**, R6823 (1996).

[36] B. J. Hickey, M. A. Howson, S. O. Musa, G. J. Tomka, B. D. Rainford, and N. Wiser, J. Magn. Magn. Mater. **147**, 253 (1995).

[37] G. Bertotti, *Hysteresis in Magnetism* (Academic, San Diego, 1998), p. 3.